AD-A088 936 NAVAL RESEARCH LAB WASHINGTON DC F/G 2 /3
ON THE MICROWAVE INTERACTION WITH MATTER AND MICROWAVE BREAKDOW-- TC(U)
SEP 80 A W ALI, T COFFEY
UNCLASSIFIED NRL-MR-4320 NL

END
DATE
FILMED
10 80
DTIC

14 NRL-MR-4320

SECURITY CLASSIFICATION OF THIS PAGE (When Data Entered)

REPORT DOCUMENTATION PAGE		READ INSTRUCTIONS BEFORE COMPLETING FORM
1. REPORT NUMBER: NRL Memorandum Report 4320 (9)	2. GOVT ACCESSION NO.: AD-A088936	3. RECIPIENT'S CATALOG NUMBER
4. TITLE (and Subtitle): ON THE MICROWAVE INTERACTION WITH MATTER AND MICROWAVE BREAKDOWN OF AIR (6)		5. TYPE OF REPORT & PERIOD COVERED: Interim report on a continuing NRL problem
		6. PERFORMING ORG. REPORT NUMBER
7. AUTHOR(s): (10) A. W. Ali [redacted] T. Coffey		8. CONTRACT OR GRANT NUMBER(s): (16) F34
9. PERFORMING ORGANIZATION NAME AND ADDRESS: Naval Research Laboratory, Washington, D.C. 20375		10. PROGRAM ELEMENT, PROJECT, TASK AREA & WORK UNIT NUMBERS: (17) 67-0868-0-0, 62734N, OF34372501
11. CONTROLLING OFFICE NAME AND ADDRESS: NAVAIR Systems Command, Dept. of the Navy, Washington, D.C. 20361 (11) 12		12. REPORT DATE: Sep[redacted]80
		13. NUMBER OF PAGES: 42
14. MONITORING AGENCY NAME & ADDRESS (if different from Controlling Office): (12) 43		15. SECURITY CLASS. (of this report): UNCLASSIFIED
		15a. DECLASSIFICATION/DOWNGRADING SCHEDULE

16. DISTRIBUTION STATEMENT (of this Report)

Approved for public release; distribution unlimited.

17. DISTRIBUTION STATEMENT (of the abstract entered in Block 20, if different from Report)

18. SUPPLEMENTARY NOTES

19. KEY WORDS (Continue on reverse side if necessary and identify by block number)

Microwave interaction
Air breakdown
Metal vaporization

20. ABSTRACT (Continue on reverse side if necessary and identify by block number)

The interaction of microwave radiation with matter (good conductors and dielectrics) is discussed. Approximate relations are given for the power necessary to vaporize surfaces of these materials. Calculations are also presented for threshold power for air breakdown at microwave frequencies.

DD FORM 1 JAN 73 1473 EDITION OF 1 NOV 65 IS OBSOLETE
S/N 0102-LF-014-6601

251950 gu

SECURITY CLASSIFICATION OF THIS PAGE (When Data Entered)

CONTENTS

ON THE MICROWAVE INTERACTION WITH MATTER AND MICROWAVE BREAKDOWN OF AIR

1. PROPAGATION OF ELECTROMAGNETIC RADIATION IN AN ATMOSPHERE

1.1 Introduction

The propagation of electromagnetic radiation in the atmosphere and in outer space is of considerable interest in many areas of applied physics. The most prominent research field for radiation propagation is the communication sciences. The propagation of radiation in the atmosphere can be quite complex. This complexity is due to a variety of physical processes which occur during the interaction of radiation with atmospheric constituents. Furthermore, the electromagnetic radiation constitutes a large spectrum of frequencies which range from x-rays to radio waves, with each frequency interacting with the atmosphere in a different manner.

In this report we restrict ourselves to microwaves and will discuss some of their applications and propagation aspects in the atmosphere. One application utilizes microwave radiation to interact with a target in the atmosphere or in outer space. Depending on the intensity of the incident radiation, the target can be heated to a desired temperature, melted or vaporized. These results can be accomplished by focussing the microwave radiation on the target of interest. Furthermore, microwave radiation can be focussed on a given area in the atmosphere to create a degree of ionization which depends critically on the wavelength of the incident radiation.

Manuscript submitted July 1, 1980.

The creation of an ionized medium in the atmosphere has several interesting consequences. One of these is that the ionized air acts as a reflector, or an attenuator, of incoming radiation. Another, is that the ionized air is a source of radiation in the visible and infrared which could adversely impact sensors operating in the visible or the infrared.

These applications depend on the understanding of the interaction of the microwave radiation with targets. This interaction determines the radiation intensity required for effecting a desired change. This is discussed in Chapter 2 of this report. Transport of high intensity radiation requires a knowledge of the air breakdown threshold power. This is discussed in Chapter 3 of this report.

1.2 Radiation Intensity and Focussing

The applications of microwave radiation discussed in Section 1.1 require, in general, a high intensity radiation. One of the well-known techniques for obtaining high intensity radiation is to focus coherent radiation on a small area. The smallest area on which radiation can be focussed is determined by the diffraction effects. Such techniques have resulted in laser intensities in 10^{17} watts per cm^2 in the optical region. Generally, the divergence of a coherent radiation with a wavelength, λ, emanating from an aperture of diameter, d, is

$$\delta\,\theta \approx \frac{\lambda}{d} \qquad 1.1$$

If the focussing distance is R_f, then the radius of the spot size is

$$r_s \simeq \frac{\lambda}{d} R_f \qquad 1.2$$

Thus, for example, to focus the microwave radiation over an area with a diameter of 100 cm at a distance of 10 km, Equation 1.2 requires that the antenna aperture be 10^4 times the radiation wavelength ($d = 10^4\lambda$).

The approximate relation given in Equation 1.2 can be utilized to calculate the desired intensity at the target and the corresponding intensity at the antenna. In a more realistic manner, however, the attenuation of the radiation in the atmosphere should be considered along with the intensity distribution on the focussed spot.

The semi quantitative relation of Equation 1.2, coupled with the approximate relations developed in Chapters 2 and 3 provide a coherent approach to the understanding of certain propagation aspects of the microwave radiation.

1.3 Higher Intensity and Coupling Considerations

The interaction of the microwave radiation with a target and its air breakdown are two aspects of interest discussed in this report. Both problems are considered on theoretical grounds based on certain simplifying assumptions. However, these problems require experimental verification as well as more detailed and self-consistent theoretical and computer modelling. These requirements are necessitated by the lack of information, especially when high microwave power densities ($P > 10^6$ watts) are considered. Experimental breakdown studies by pulsed microwave radiation have not been carried out for any power level beyond 10^6 watts. Higher power densities, e.g., 10^9 watts are becoming available and would, in principle, enhance the local effective electric field by a factor of 30 which clearly will change the free electron distribution and hence the ionization condition and the emission characteristics of the ionized air. In the area of the interaction with a target, the high intensity microwave radiation may produce

a vaporized, ionized, medium on the target surface. Several interesting questions arise in this aspect. For example, what is the role of this atomized region in terms of coupling the radiation energy into the target? Does the ionized region become a source of energy that impacts the target? To answer these and other questions, further experimental and theoretical considerations are in order.

2. IRRADIATION OF A TARGET BY ELECTROMAGNETIC RADIATION

2.1 Introduction

The irradiation of a target, whether a conductor or a dielectric material, by electromagnetic radiation will raise the target temperature and may crack, melt or vaporize it. The physical changes depend on the intrinsic characteristics of the material and the amount of energy it absorbs. In this section we discuss these physical changes and the amount of power required to initiate them. This can be accomplished by calculating the target temperature as a function of time and its dependence on the power and the wavelength of the incident radiation. The target temperature is obtained from an analytic solution of the heat equation in one dimension. From this analytic solution, approximate expressions for the surface temperature are obtained and are utilized for quantitative estimates of the power required to vaporize a target.

When the radiation is incident on a target, a certain amount of the energy is reflected. The reflectivity of the target, obviously, influences the total incident radiation required to vaporize a target. In this chapter we give a simple relation for the reflectivity of good conductors as a function of the wavelength of the incident radiation. This will be incorporated in the approximate target temperature equation to give the total power necessary to induce the physical changes on a target.

2.2 Heat Equation and the Target Temperature

The equation describing the heat flow into a solid target is[1]

$$\underline{K}\, \nabla^2 T + Q = \rho\, C_p \frac{dT}{dt} \tag{2-1}$$

where $\underline{K}$ is the thermal conductivity of the target, ρ its density, C_p is its specific heat at constant pressure, Q is the rate of the energy input per unit volume and T is the temperature. The above equation can be rewritten as

$$\nabla^2 T + \frac{Q}{\underline{K}} = \frac{1}{k}\frac{dT}{dt} \tag{2-2}$$

where k is the thermal diffusivity of the target and is defined as $\frac{\underline{K}}{\rho C_p}$ which is the ratio of the thermal conductivity to the heat capacity of the target.

Consider the solution to Equation (2-2) for a uniform irradiation incident perpendicular to the surface of a semi-infinite slab of material. We seek a solution in one dimension for an incident power which is absorbed as it traverses the target according to $Q=Q_o\, e^{-\alpha x}$ where α is the absorption coefficient of the target whose surface boundary is at x=o. Assuming that the target temperature is T=o at t=o, the solution to Equation (2-2) is

$$\begin{aligned} T(t,x) = \alpha \Bigg\{ & \frac{2Q_o}{\underline{K}} (kt)^{\frac{1}{2}} \text{ i erfc } \frac{x}{2(kt)^{\frac{1}{2}}} - \frac{Q_o}{\alpha\, \underline{K}}\, e^{-\alpha x} \\ & + \frac{Q_o}{2\underline{K}\,\alpha^2}\, e^{\alpha^2 kt - \alpha x} \cdot \text{erfc}\left[\alpha (kt)^{\frac{1}{2}} - \frac{x}{2(kt)^{\frac{1}{2}}}\right] \\ & + \frac{Q_o}{2\underline{K}\,\alpha^2}\, e^{\alpha^2 kt + \alpha x} \cdot \text{erfc}\left[\alpha (kt)^{\frac{1}{2}} + \frac{x}{2(kt)^{\frac{1}{2}}}\right] \Bigg\} \end{aligned} \tag{2-3}$$

where Q_o is the absorbed power and

$$i\ \text{erfc}\ a = \int_a^\infty \text{erfc}\ y\ dy$$

$$\text{erfc}\ a = \frac{2}{\sqrt{\pi}} \int_a^\infty e^{-y^2}\ dy$$

$$i\ \text{erfc}\ o = \frac{1}{\sqrt{\pi}}$$

$$i\ \text{erfc}\ \infty = o$$

The surface temperature of the target can be obtained immediately from Equation (2-3) by setting x=o, that is;

$$T(t,o) = \frac{Q_o}{\alpha \underline{\bar{K}}} \left\{ \left(\frac{4\alpha^2 kt}{\pi} \right)^{\frac{1}{2}} - 1 + e^{\alpha^2 kt} .\ \text{erfc}\ (\alpha^2 kt)^{\frac{1}{2}} \right\} \qquad (2\text{-}4)$$

The solution to Equation (2-2) was obtained under the assumption that the thermal conductivity and the thermal diffusivity of the target are constant with temperature. This is reasonable for metals where these coefficients change slightly with the target temperature. Table 1 gives the thermal conductivity and the heat capacity of copper as a function of temperature[2].

Table 1

Temp	0 °c	100 °c	300 °c	700 °c
$\underline{\bar{K}} \left(\frac{\text{Watt}}{\text{cm}\ ^\circ\text{c}}\right)$	3.85	3.82	3.76	3.5
$\underline{\bar{K}}/k \left(\frac{\text{Joule}}{\text{mole}\ ^\circ\text{c}}\right)$	24.6	24.9	25.2	27.7

However, the thermal conductivity is reduced by a factor of two when

the solid is melted.

2.2 The Reflectivity of the Target

In Equations (2-3) and (2-4), Q_o represented the power absorbed in the target which generates the heating and the rise in the target temperature. However, when radiation is incident on any surface, part of the radiation is transmitted while another part is reflected. Therefore, it is of interest to know the reflectivity or the transmittance of the target for each wavelength in order to obtain the total incident radiation on the target. Therefore, if we defined $\underline{P}$ as the total incident power, then

$$Q_o = (1-R)\ \underline{P} \tag{2-5}$$

where R is the reflectivity of the target.

Consider the case of *normal incidence* of electromagnetic radiation on the surface of a good conductor. The transmittance of a good conductor is related to the skin depth, δ, as[3]

$$1-R = \frac{4\pi}{\lambda}\,\delta \tag{2-6}$$

where λ is the wavelength of the incident radiation and

$$\delta = \frac{c}{\sqrt{2\pi\mu\omega\sigma}} \tag{2-7}$$

In Equation (2-7), μ is the permeability and σ is the electrical conductivity and ω is the angular frequency of the incident radiation.

Using Equation (2-7) into (2-6), one obtains

$$1\text{-}R = 3.46 \times 10^{5} \frac{1}{\sqrt{\mu \lambda \sigma}} \qquad (2\text{-}8)$$

In general, the electrical conductivity of a good conductor[3,4] is $\sigma \sim 10^{17}$ sec^{-1} while the permeability is ~ 1 (for non magnetic material). For radiation at λ=3 cm, the amount absorbed in a conductor is $\sim 6 \times 10^{-4}$. In Figure 2.1 are shown 1-R values for copper, Cu, and aluminum, Al, over a wavelength range 0.01-3 cm. For example, at λ=3 cm, the amount of radiation transmitted into Cu and Al are 2.3×10^{-4} and 3.4×10^{-4}, respectively. On the other hand, for carbon, the transmittance at λ=3 cm, is 8×10^{-3} which is larger by an order of magnitude compared to that for Cu and Al. This is because the electrical conductivity of carbon[4] is 6.3×10^{14} sec^{-1} which is lower by two orders of magnitude compared to good conductors.

For dielectric materials on the other hand, assuming normal incidence, the reflectivity is[5]

$$R = \left(\frac{n-1}{n+1}\right)^2 \qquad (2\text{-}9)$$

where n is the index of refraction. Dielectrics such as epoxy cast resin, polyethylene and rubber, have index of refractions[6] of n=1.7 for the visible light. For longer wavelength ($\lambda \approx 10$ cm), their refractive indices[7] range from 1.4 to 1.7 implies small reflectivities. This implies that in a sense, less total incident power will be required to crack, heat or vaporize dielectric materials.

2.3 Vaporization of a Solid

In Section 2.2 an analytic solution was given for the temperature at any point inside a solid and as a function of time (see Equations 2-3 and 2-4). These equations can be utilized to heat a target to any desired temperature knowing the power of the incident radiation. However, certain approximate expressions for the target temperature can be obtained. From these expressions one can obtain quantitative estimates for the power needed to melt or vaporize a target.

Consider the surface temperature of a target as given by Equation (2-4). An approximate expression can be obtained for early times when $\alpha^2 kt \ll 1$ or $\alpha^2 k \ll \frac{1}{t}$. In this case,

$$T\ (t,o) = (1-R)\ \alpha.\ \frac{k}{K}\, P.t, \tag{2-10}$$

where use is made of Equation (2-5). The concept of an early time can be clarified if one defines

$$t_o = \frac{1}{\alpha^2 k} = \frac{\delta^2}{k} \tag{2-11}$$

where the absorption length is of the order of the skin depth and that t_δ is the time required for heat to diffuse a distance of δ. Thus for any time $t < t_\delta$, Equation (2-10) can be used to calculate the power needed to raise the target surface to melting or vaporization temperatures. The skin depth for good conductors is $\sim 10^{-5}$cm at $\lambda = 3$ cm and $k \sim 1$ cm^2/sec, thus $t_\delta \approx 10^{-10}$sec. However, of more interest is heating a target for longer times.

Thus we would like to obtain an approximate relation from (2-3) and (2-4) for times t where

$$t_\delta < t < t_\ell \tag{2-12}$$

Here $t_\ell = \frac{\ell^2}{k}$ with ℓ being the target thickness which is usually very large compared to the skin depth ($\ell >> \delta$). The concept of a long time, here, implies that heat has diffused beyond a skin depth but that the temperature of the back surface of the target is unchanged. Such an approximation yields

$$T(0,t) = \frac{2(1-R)P}{\overline{K}}\left(\frac{kt}{\pi}\right)^{\frac{1}{2}} \tag{2-13}$$

which we will use to estimate the total power needed to vaporize a skin depth of the target material. This is done by ignoring the liquid phase of the solid which is valid since the latent heat of fusion is much smaller than the latent heat of vaporization. The heat of fusion is also much smaller than the quantity of heat needed to raise the target to vaporization temperature.

The time to reach vaporization temperature for any power level can be obtained by rewriting Equation (2-13), that is

$$t_V = \frac{\pi}{4}\frac{\overline{K}^2}{k}\frac{T_V^2}{(1-R)^2}\frac{1}{P^2} \tag{2-14}$$

It is obvious from Equation (2-14) that higher power levels are needed if one desires shorter times to reach vaporization temperatures.

2.3.1 Applications to Good Conductors

Consider copper where $\underline{K}$ = 3.85 watt cm^{-1} $°c^{-1}$, k = 1.1 cm^2 sec^{-1} and T_V is 2300 °c [6]. The time to reach vaporization temperature is

$$t_V = \frac{5.5 \times 10^7}{(1-R)^2 \; P^2}$$

where P is in watts cm^{-2}. This relation is illustrated in Figure 2.2 for several wavelengths of the incident radiation. It is clear from this Figure that vaporization temperature is reached faster and at a lower power level for shorter wavelengths of the incident radiation.

Another interesting application of Equation (2-13) is when the incident power duration is specified and one is then interested in the power needed to vaporize the solid. Using the values of $\underline{K}$, k and T_V given earlier for copper, Equation (2-13) reduces to

$$P(1-R) = \frac{7.5 \times 10^3}{\sqrt{t}} \qquad (2\text{-}15)$$

Now consider an incident radiation at λ=3 cm and t=10^{-2} sec, with 1-R being 2.7 X 10^{-4} one needs P=2.8 X 10^8 watts/cm^2 to heat copper to its vaporization temperature. This is equivalent to 2.8 X 10^{12} watts/m^2. The analysis leads to P=1.5 X 10^{12} watts/m^2 for Al where $\underline{K}$ = 2.37 watt cm^{-1} $°c^{-1}$, k=1.0 cm^2 sec^{-1} and T_V=2460 °c [6]. These power levels are in agreement with previous calculations reviewed in Reference (7).

Once the vaporization temperature is reached, the rate of the material removal and the vaporized depth of the material can be estimated. The rate of vaporization or the surface ablation velocity, V_a,

can be expressed[2], as

$$V_a = \frac{(1-R)\ P}{\rho L_v + \rho C_p T_v} \tag{2-16}$$

where heat losses due to convection and conduction are ignored. In Equation (2-16), ρ is the density of the solid, L_v is the latent heat of vaporization. Thus the vaporized depth, ℓ_v, is obtained from Equations (2 - 16) for the velocity and Equation (2-14) for the vaporization time,

$$\ell_v = V_a t_v \tag{2-17}$$

For copper, L_v = 4000 J/gm, ρ = 7 gm/cm^3 and $C_p \approx$ 0.09 cal gm^{-1} c^{0-}. Using these values into Equations (2-16) and (2-17) with a power of 2.8×10^8 watt/cm^2 at λ = 3 cm, one obtains $\ell_v \approx$ 0.025 cm. Thus to vaporize one centimeter depth of a copper target, one needs 40 pulses of 10^{-2}sec duration for each pulse. This estimate assumes that the energy is coupled to the target in the same way for each subsequent pulse. Such an estimate may be appropriate for a moving target. For a still target, however, the amount of surface material vaporized after the first pulse may act as an absorber of the incident energy in the pulses that follow. This may decouple the incident radiation from the target. However, further heating of the vaporized region could result in a plasma whose radiation in shorter wavelengths is absorbed by the target. Obviously the problem is rather complex and requires a comprehensive treatment.

2.3.2. Application to Carbon

The electrical conductivity of carbon is 6.3×10^{14} sec^{-1} which is lower by two orders of magnitude compared to that for good

metallic conductors. This characteristic makes carbon a better absorber of radiation compared to good conductors. For example, 1-R for carbon is 8×10^{-3} at λ=3 cm compared to 2.7×10^{-4} for copper. For this reason it is of interest to apply the approximate vaporization relations of Section 2.3 to carbon.

Using Equation (2-13) for carbon where $\overline{K}$ = 0.24 watt cm^{-1} °c^{-1}, k=0.16 cm^2 sec^{-1} and T_V = 4830 °c ,[4] we obtain

$$P = \frac{2.6 \times 10^2}{(1-R)\sqrt{t}} \tag{2-18}$$

which yields P=3.2×10^6 watts/cm^2 for λ=3 cm and 1-R=8×10^{-3}. This value of power to raise carbon to its vaporization temperature is small by two orders of magnitude compared to that for copper.

2.3.3 Application to Dielectric Material

The characteristics of the dielectric materials are different than those of conductors. Therefore, it is of interest to consider these materials under the impact of electromagnetic radiation. To apply the equations developed earlier for solids, one needs the amount of radiation transmitted into the solid, i.e. the quantity 1-R. For the dielectric materials the reflectivity for normal incidence is defined by Equation (2-9) which depends on the index of refraction. In Table 2, the dielectric constant[8] for several plastics are given as a function of the radiation frequency.

Table 2

Plastics	$\nu(H_z)$ 10^3	10^6	10^8	$3X10^9$	$2.5X10^{10}$
Epoxy Resin	3.67	3.62	3.35	3.09	
Polyethylene	2.26	2.26	2.26	2.26	2.26
Polyhexamethylene - adipamide (Nylon)	3.5	3.14	3.0	2.84	2.73
Polytetrafluoroethylene (Teflon)	2.1	2.1	2.1	2.1	2.1

For the region of interest, the dielectric constants for these plastics change very slightly with the radiation frequency. Therefore, the index of refraction is also constant with respect to the incident wavelength. The corresponding values of n for polyethylene and teflon are 1.5 and 1.45, respectively. This implies that 1-R for these two plastics are 0.96 and 0.97, which means that they are practically transparent to microwave and radio frequencies. Table 3 gives the necessary data[9] on polyethylene and teflon.

Table 3

	Density gm/cm^3	Thermal Conductivity 10^{-4} $cal/sec/cm^2/1°c/cm$	Specific Heat $cal/°c/gm$
Polyethylene - oxide based	1.28	3.8	0.32
Teflon	2.17	6.0	0.25

These data can be used to obtain the thermal diffusivities which are 9.2×10^{-4} cm^2/sec and 1.1×10^{-3} cm^2/sec for polyethylene and teflon, respectively. With the information in Tables 2 and 3 on the

transmittance, thermal conductance and thermal diffusivity, we can estimate the power needed to decompose these dielectrics. However, one must estimate the absorption coefficient or the skin depth in order to apply the approximate relations given in Equations (2-10) and (2-13). The absorption coefficient for teflon at $\lambda = 0.005$ cm is[10] 200 cm^{-1} which implies a skin depth of 5×10^{-3} cm. The time for heat to diffuse a skin depth is 0.025 sec. Thus one can utilize Equation (2-13) for times longer than 0.025 sec, say 2×10^{-1}sec. Using the relevant data for teflon into Equation (2-13), where the decomposition temperature is[11] 350°C, one obtains

$$P \approx \frac{15}{\sqrt{t}}$$

This implies that for a pulse duration of 10^{-1}sec one needs ≈47 watts/cm^2 to decompose teflon with a radiation at $\lambda = 5 \times 10^{-3}$cm. At longer wavelengths, however, the absorption coefficients are smaller and can be obtained if the loss angle or power factor are known. The absorption coefficient can be expressed as[12]

$$\alpha = \frac{\pi \tan\delta}{\lambda} n, \quad \tan\delta = 0.0001 \text{ to } 0.05$$

and

$$\alpha = \frac{2\pi}{\lambda} n \sqrt{\frac{\sqrt{1 + \tan^2\delta} - 1}{2}}, \quad \tan\delta = 0.05 \text{ to } 50$$

where $\tan\delta$ is the loss factor. For polyethylene the loss factor is ≈ 6×10^{-4} for λ from 3 cm to 10 cm. This implies that the absorption coefficient is small and the skin depth large in these wavelength ranges and one must select the appropriate time and Equations to estimate the power needed to decompose these dielectrical material.

2.3.4. Remarks on Target Heating

When a target surface is irradiated by a sufficient flux from a radiation source, certain amount of the surface material is vaporized. This vaporized layer has an atomic nature and its absorbing characteristics are very different than those of a solid and a polished surface. The vaporized layer absorbs the incoming radiation and may decouple it from the target surface. Thus the calculations presented here are, in principle, applicable to a moving surface whereupon the vaporized layer does not pose a decoupling problem. However, a comprehensive treatment requires a detailed time dependent model calculation which takes into consideration the vaporized layer and its effects on the heating and vaporization of target material as well as the hydrodynamic effects.

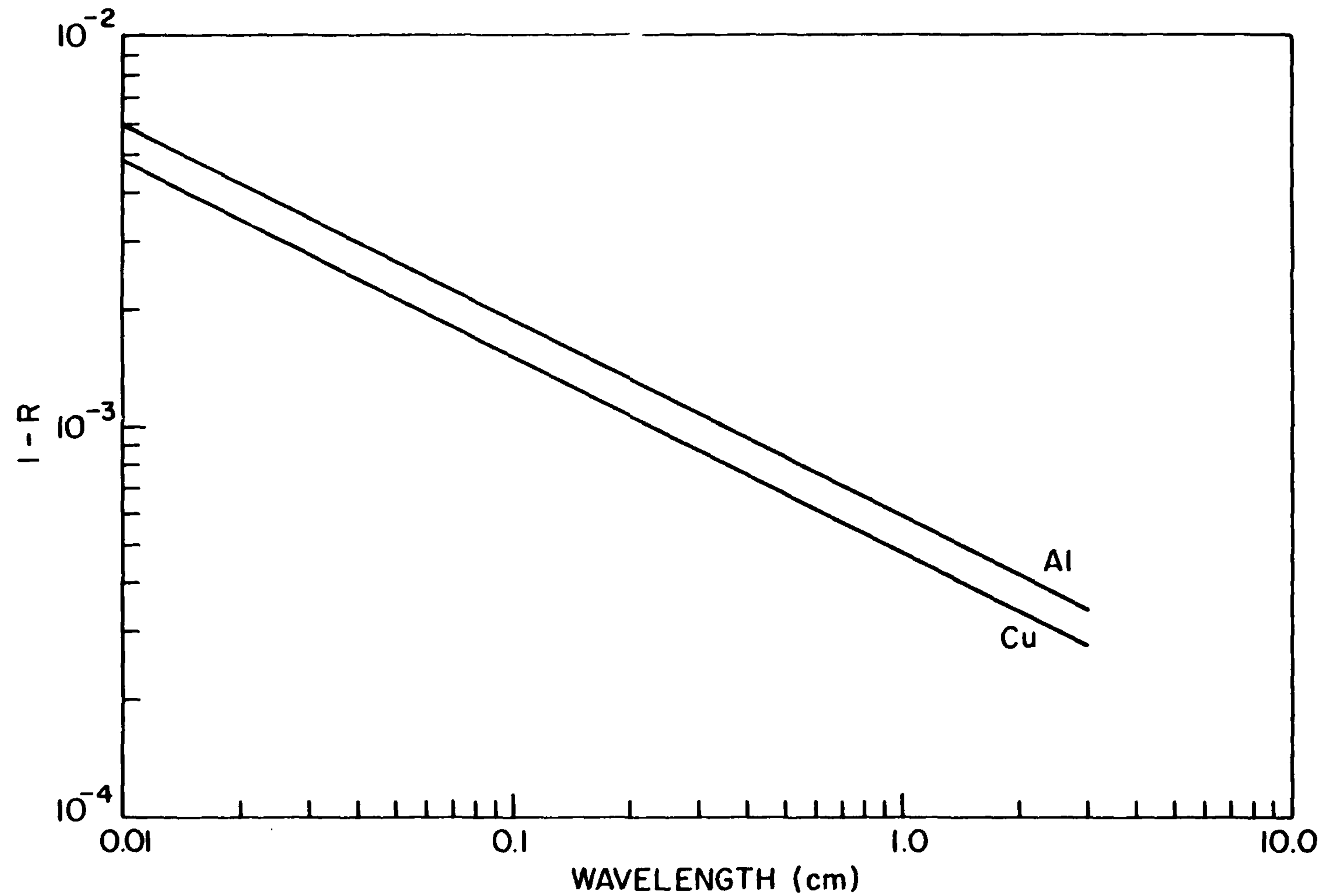

Fig. 2.1 — The transmittance of aluminum and copper as a function of wavelength

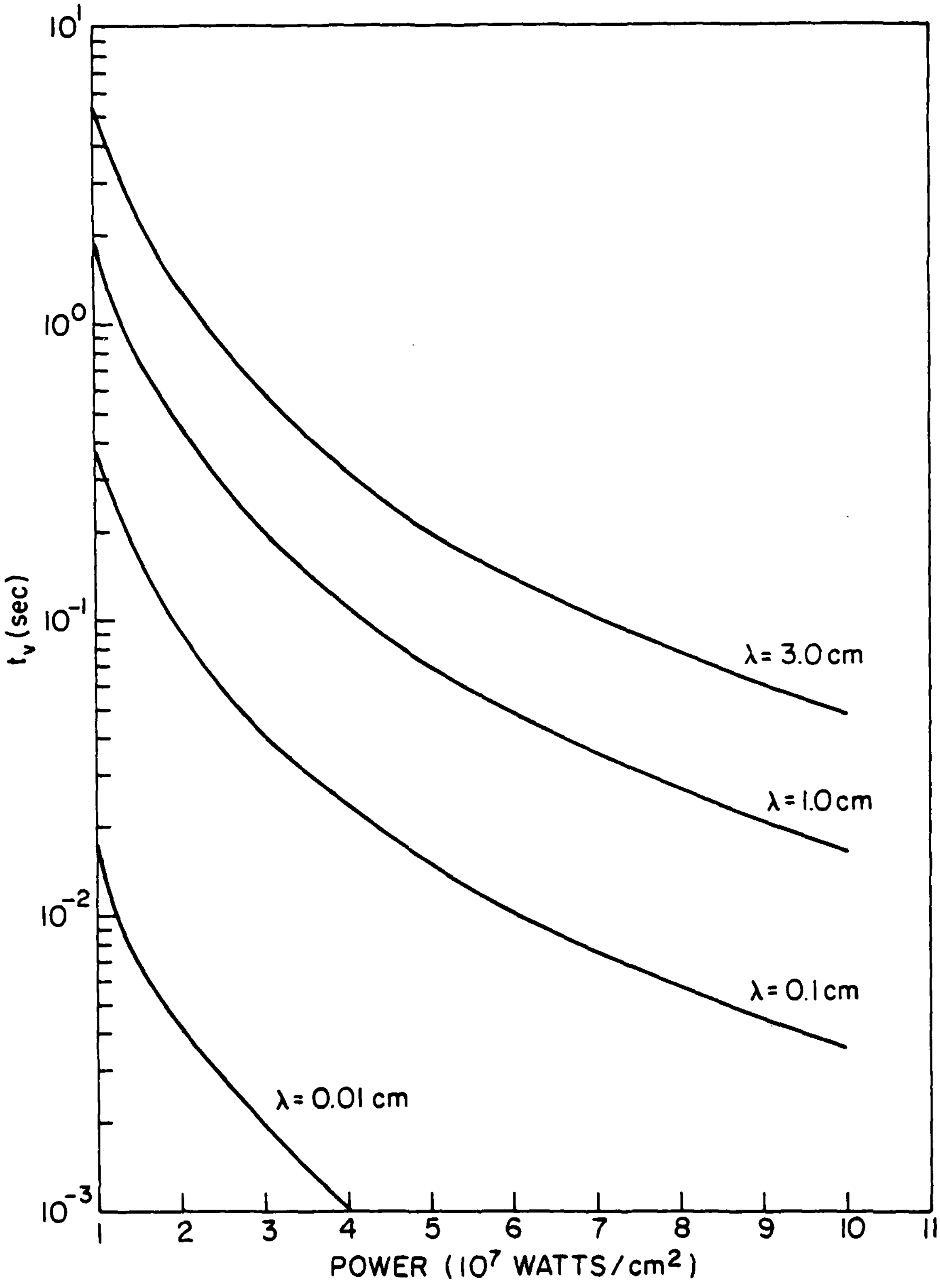

Fig. 2.2 — The time to reach vaporization for a copper surface as a function of incident power for several wavelengths

3. AIR BREAKDOWN

3. Introduction

In Section Two of this report, quantitative relations and estimates were given for heating and vaporization of solid materials under the impact of electromagnetic radiation. However, radiation, generally, propagates in a medium, such as air, before reaching the point of interest. Propagation, especially in air, is accompanied by several physical processes which affect adversely the transportation of radiation. One of the important processes that limits the propagation of radiation in air is the air breakdown which will be discussed in this section. This discussion will provide quantitative relations which determine the breakdown threshold as a function of the power and the wavelength of radiation. Such information is essential in order to avoid air breakdown when radiation is transported and focussed at any desired point in space.

3.2 Air Breakdown by Electromagnetic Radiation

3.2.1 Theory of Breakdown

The breakdown in air or any other gaseous medium is exemplified by the creation of a plasma. This occurs when sufficient power from an electromagnetic source is focussed in air, whereupon the free electrons present gain energy under the influence of the intense electric fields associated with the focussed radiation. The energy gained by electrons is expended in producing more electrons by electron impact ionization culminating in cascade ionization of the gaseous medium.

There have been considerable studies of breakdown in many gase-

ous elements and in air under the influence of microwave radiation[7,13-15]. With the advent of lasers and high power Q-switched lasers, the air and gaseous breakdown studies at optical frequencies have increased considerably[16,17].

The mechanism for gas breakdown can be explained by the classical microwave breakdown theory[14], where the electron gains energy from the electric field only when it collides with an atom and the sudden change in its velocity results in the transfer of the oscillation energy into random motion. This energy gain process has been shown to correspond[18] to the quantum mechanical description of the energy gain by the free electrons from the radiation field through the free-free transitions in the field of an atom.

The rate of energy gain by the free electron under the influence of the electric field, E, of the incident radiation is

$$\left.\frac{d\epsilon}{dt}\right)_g = \frac{e^2\, E^2}{m\, \omega^2}\, \nu_c\, \frac{\omega^2}{\omega^2 + \nu_c^{\,2}} \tag{3-1}$$

where ω is the natural frequency of the oscillatory electric field, ν_c is the collision frequency of the electron with the neutral atoms. On the other hand, a simplified model for the rate of energy loss in air is

$$\left.\frac{d\epsilon}{dt}\right)_\ell = - \frac{D\,\bar{\epsilon}}{\Lambda^2} - \frac{2m}{M}\epsilon\, \nu_c - \left(\nu_i \epsilon_i + \nu_a \bar{\epsilon} + \Sigma_e \nu_e \epsilon_e\right) \tag{3-2}$$

Where D is the diffusion coefficient, Λ the diffusion length, $\bar{\epsilon}$ is the average electron energy, ν_i, ν_a and ν_e are the collision frequencies for

ionization, attachment and excitations, respectively, while ϵ_i and ϵ_e are the corresponding energies for ionization and excitations, respectively. The second term on the right hand side of Equation (3-2) represents the energy loss by electrons through elastic collisions with the neutrals. Therefore, the net energy gained by electrons is

$$\frac{d\epsilon}{dt} = \left.\frac{d\epsilon}{dt}\right)_g - \left.\frac{d\epsilon}{dt}\right)_\ell \tag{3-3}$$

Furthermore, the time development of the electron density is described by

$$\frac{dn_e}{dt} = n_e\nu_i - n_e\nu_a - n_e\frac{D}{\Lambda^2} \tag{3-4}$$

where it is obvious that electron attachment and diffusion will control the cascade ionization process and must be overcome for breakdown to occur. Two limiting cases of Equation (3-4) can be of great interest. These are the diffusion controlled and attachment controlled cases of air breakdown. At atmospheric pressure, however, the air breakdown is attachment controlled.

The condition for a cw breakdown is $\frac{dn_e}{dt} = 0$ which implies that

$$\nu_i = \nu_a + \frac{D}{\Lambda^2} \tag{3-5}$$

The diffusion coefficient can be expressed as[15]

$$Dp = 3.2 \times 10^5 \bar{\epsilon} \tag{3-6}$$

where p is the pressure in mm Hg and $\bar{\epsilon}$ is the average electron energy in units of eV. Thus for typical energies of few eV and atmospheric pressures of 760 mm, the diffusion coefficient is $D \simeq 8 \times 10^2 \left(\frac{cm^2}{sec}\right)$. This implies that the rate of diffusion from an area of 1 cm^2 is $\sim 10^3$ sec^{-1} which is very small compared to the attachment rate of electrons to O_2. This latter rate is $\sim 3 \times 10^7$ sec^{-1}. However, at higher altitudes or lower air pressures, diffusion becomes important and in certain cases even a dominant controlling factor in air breakdown.

3.2.2 Simple Air Breakdown Calculations

The air breakdown calculation, in principle, can be carried out by solving Equation (3-3) and (3-4) with the knowledge of the electron velocity distribution and the appropriate atomic processes whose rates are electron energy dependent. However, reasonable estimates (lower limits) can be obtained for the breakdown threshold power using approximate solutions. The rate of energy growth for the electron in the radiation field, Equation (3-1), can be written in terms of the incident radiation flux, I, as

$$\frac{d\epsilon}{dt} = \frac{4\pi e^2 I}{mc} \cdot \frac{\nu_c}{\omega^2 + \nu_c^2} = \frac{0.11\ I\ \nu_c}{\omega^2 + \nu_c^2} \tag{3-7}$$

where $\frac{E^2}{4\pi} = \frac{I}{c}$ was utilized ($E = 27\sqrt{I}$ (V/cm) with I in watts/cm^2. The threshold condition is obtained using Equation (3-7) assuming that energy gained by the electron is expended to ionizations and that other

loss mechanisms are ignored. Thus the energy gained by the electron during the radiation pulse, Δt, is equal to the ionization potential of the neutral, I_i, times the critical number of generations, K_{cr},

$$\int_0^{\Delta t} \frac{d\epsilon}{dt}\, dt = K_{cr}\, I_i \tag{3-8}$$

Thus the threshold power for air breakdown is

$$I_{th} = \frac{I_i\, K_{cr}\, (\omega^2 + \nu_c^{\,2})}{0.11\, \Delta t\, \nu_c} \tag{3-9}$$

For a pulsed breakdown the first electron generates another and then these generate two more electrons and so on. The growth of the electron density is described by

$$N_e = N_e(0)\, e^{\nu \Delta t} = N_e(0)\, 2^{K_{cr}} \tag{3-10}$$

Where ν is the net ionization rate and $N_e(0)$ is the initial density of the free electrons, generally $\sim 1\ cm^{-3}$. Furthermore, it is assumed that at the end of the radiation pulse the electron density reaches its critical value, $N_e^{\ cr}$, where

$$K_{cr} = 1.45 \log_e \left(\frac{N_e^{\ cr}}{N_e(0)} \right) \tag{3-11}$$

The critical electron density depends on the radiation wavelength that causes the air breakdown and is given by

$$N_e^{cr} = \frac{10^{13}}{\lambda^2} \qquad (3\text{-}12)$$

which is shown on Figure 3.1 for several wavelengths.

To estimate the threshold power for air breakdown under optical frequencies, Equation (3-9) can be utilized with K_{cr} values ranging from 36 to 40. Using $K_{cr} = 40$ and $I_i = 14.8$ eV for the average ionization potential of air molecules in Equation (3-9) results in

$$I_{th} = 8.6 \times 10^{-16} \frac{\omega^2 + \nu_c^2}{\Delta t\, \nu_c} \text{ (watts/cm}^2\text{)} \qquad (3\text{-}13)$$

The collision frequency can be estimated[19] to be $\nu_c = 5.3 \times 10^9$ p where p is the air pressure in Torrs, therefore, Equation (3-13) reduces to

$$I_{th} = \frac{8.6 \times 10^{-16}}{\Delta t} \frac{\omega^2 + (5.3 \times 10^9\ p)^2}{5.3 \times 10^9\ p} \qquad (3\text{-}14)$$

For optical region $\omega \simeq 10^{16}$ which is much larger than ν_c, one obtains for air at atmospheric pressure a breakdown threshold power of 2×10^{10} (watts/cm^2) using a pulse with duration of 10^{-6} sec. This value is of the same order but lower by a factor of three compared to the breakdown threshold power obtained experimentally[20], indicating that the classical approach can explain the breakdown process. Thus the breakdown calculations require the interrelation of many factors which are the ionization rate, the energy loss rate, the average electron energy, the electric field and finally, the threshold power for breakdown. This requires a more detailed analysis which is carried out in the next section for microwave breakdown of air.

3.2.3 Calculation of Air Breakdown by Microwave Radiation

Approaches[21,22] to air breakdown calculations can start with the knowledge of the ionization rate of air, ν_i, which generally is expressed as $\frac{\nu_i}{p}$. This quantity depends on the electron energy which in turn depends on the critical electric field, $\frac{E_e}{p}$. For a Maxwellian electron velocity distribution and for an average electron energy of $\bar{\epsilon} \leq 20$ eV, the following relation for $\frac{\nu_i}{p}$ has been obtained[22]

$$\frac{\nu_i}{p} = 2.5 \times 10^7 \left[5.6\ (\bar{\epsilon})^{1/2} + 0.6\ (\bar{\epsilon})^{3/2}\right] \mathrm{Exp}\left(-\frac{18.75}{\bar{\epsilon}}\right) \qquad (3\text{-}15)$$

where it is assumed that in air ionization is basically from oxygen molecule ($I_i \simeq 12.5$ eV). Furthermore, an empirical relation[22] has also been found between $\bar{\epsilon}$ and $\frac{E_e}{p}$ where

$$\bar{\epsilon} \simeq 0.0675\ \frac{E_e}{p} \qquad (3\text{-}16)$$

This relation utilized into (3-15) yields

$$\frac{\nu_i}{p} = 2.5 \times 10^7 \left[1.45\left(\frac{E_e}{p}\right)^{1/2} + 0.01\left(\frac{E_e}{p}\right)^{3/2}\right] \mathrm{Exp}\left(\frac{-278}{\frac{E_e}{p}}\right) \qquad (3\text{-}17)$$

which is shown in Figure 3.2. Thus the problem is a simple one for air breakdown when it is attachment controlled. For cw the condition for breakdown is

$$\nu_i = \nu_a \qquad (3\text{-}18a)$$

or equivalently

$$\frac{\nu_i}{p} = \frac{\nu_a}{p} \tag{3-18b}$$

The value of $\frac{\nu_a}{p}$ is known and thus one can obtain $\frac{E_e}{p}$ from Equation (3-17). However, for pulsed breakdown, the ionization rate must be high enough so that the electron density reaches its critical value within the duration of the radiation pulse. This requires that

$$\frac{\nu_i}{p} - \frac{\nu_a}{p} = \frac{1}{p\Delta t} \log_e \frac{N_e^{cr}}{N_e(0)} \tag{3-19a}$$

or

$$\frac{\nu_i}{p} - \frac{\nu_a}{p} = \frac{1}{p\Delta t} \log_e \left[10^{13} / \lambda^2 \cdot N_e(0)\right] \tag{3-19b}$$

where we have utilized Equations (3-10 and (3-12). Thus for any wavelength, Δt and p we can obtain $\frac{\nu_i}{p}$. From Figure 3.2 or Equation (3-17) we obtain the corresponding $\frac{E_e}{p}$ and hence the threshold breakdown power. Using λ = 3 cm, p = 760 mm, $\Delta t = 10^{-6}$ and $N_e(0) = 1$ in Equation (3-19b) we obtain $\frac{E_e}{p} \sim 30$ volts/cm Torr.

An application of Equation (3-19b) with $N_e(0) = 1$ for a fixed pulse duration ($\Delta t = 10^{-6}$ sec) is shown in Figure 3.3 for several different wavelengths. In this Figure $\frac{\nu_i}{p}$'s are given as a function of air

pressure (altitude). The corresponding effective electric fields as a function of pressure (altitude) are shown in Figure 3.4. In this figure the independence of the electric field on the radiation wavelength with increasing pressure, is a manifest of the attachment controlled domain for breakdown.

3.2.4 Air Breakdown Calculation With Diffusion Effect

The calculation in Section 3.2.3 of this report was carried out ignoring the diffusion effect. However, when the density of air is reduced, diffusion may become an important factor in air breakdown and, therefore, it has to be considered. In this section we present air breakdown calculations by including the diffusion effects phenomenologically. In addition, we present the effect of the radiation pulse width on the breakdown thresholds.

The criterion for a cw breakdown is

$$\frac{\nu_i}{p} = \frac{\nu_a}{p} + \frac{D}{P\Lambda^2} \tag{3-20}$$

which is equivalent to Equation (3-5). For a pulsed condition, however, the criterion for breakdown is

$$\frac{1}{P}\left(\nu_i - \nu_a - \frac{D}{\Lambda^2}\right) = \frac{1}{P\Delta t}\log_e\left(N_e^{cr}/N_e(0)\right) \tag{3-21}$$

This implies that two other parameters have to be known in order to calculate the critical field. These are, D and Λ. The diffusion coefficient is related to E_e/P according to

$$DP = \left[29.0 + 0.9 \frac{E_e}{P} \right] X\ 10^4 \qquad (3\text{-}22)$$

and Λ is generally a characteristic length of the breakdown geometry and can be estimated. In Figure 3.5 we present breakdown threshold power calculations as a function of pressure for several wavelengths of the incident radiation. These calculations were carried out with Λ=0.75 cm and $\Delta t = 3X10^{-6}$ sec. It is obvious from this Figure that the threshold breakdown power increases with increased frequency of the incident radiation. However, these calculations were repeated for a shorter pulse width i.e. $\Delta t = 3X10^{-7}$ sec to demonstrate the effect of shorter pulse duration. These latter results are shown in Figure 3.6 where it is obvious that the reduction in the radiation pulse width, for each wavelength, results in higher breakdown threshold power.

A final remark is in order in regards to breakdown calculations. Free electrons in ionized air decay through recombination in addition to attachment and diffusion from the ionized region. For ionization by microwave radiation ($\lambda \geq 1$ cm), electron densities are $n_e \leq 10^{13}$ cm^{-3} where recombination will proceed through the process of dissociative recombination which depends on the electron temperature[22]. The dissociative recombination rate coefficients are 1.8 x 10^{-7} cm^3/sec and 2.0 x 10^{-7} cm^3/sec for N_2^+ and O_2^+, respectively. Therefore, one can always compare this with the attachment and diffusion rates to see whether recombination should be included. The three-body attachment of electrons and the dissociative attachment with O_2 are also tempera-

ture dependent. The three-body process has a rate coefficient[24] of 1.8 x 10^{-30} cm^6/sec and 1.0 x 10^{-31} cm^6/sec when the third bodies are molecular oxygen and nitrogen, respectively. Such coefficients will give a combined attachment rate at the sea level of 6 x 10^7 sec^{-1}. This implies that the lifetime of a free electron due to the three-body attachment is in 1.6 x 10^{-8} seconds. This should be compared with a lifetime of 5 x 10^{-7} seconds due to dissociative recombination for an electron density of $n_e = 10^{13}$ cm^{-3}. For lower electron densities, lifetimes due to dissociative recombinations, become much longer. However, when the neutral densities are reduced below one atmosphere, there may be regions and electron densities of interest where recombination should be included. These rates should also be compared with the diffusion rate (see Equation 3-22) which generally becomes very high at very low pressures.

REFERENCES

1. H. S. Carslaw and J. C. Jaeger, "Conduction of Heat in Solids", 2nd Ed. (Clarendon, Oxford, 1959).
2. J. F. Ready, "Effects of High-Power Laser Radiation", Academic Press, New York (1971).
3. J. D. Jackson, "Classical Electrodynamics", John Wiley & Sons, New York (1967).
4. "Metals Handbook", 1948 Edition, T. Lyman, Ed., American Society for Metals, Cleveland (1954).
5. F. A. Jenkins and H. E. White, "Fundamentals of Optics", McGraw-Hill (1957).
6. "Handbook of Chemistry and Physics", 50th Edition, R. C. West, Ed., The Chemical Rubber Co., Cleveland, Ohio (1969).
7. (a) "Summary Review of Project Comet", Defense Research Corporation, Technical Project #RADC-TR-66-320 (1966) SR. (b) "Nanosecond Pulse Breakdown in Gases" by P. Felsenthal & J. M. Proud, Rome Air Development Center Technical Report No. RADC-TR-65-142, June 1965.
8. "Reference Data for Radio Engineers", 5th Edition, H. P. Westman, Ed., Howard W. Sams & Co., Inc., New York (1972).
9. "Thermal Conductivities of Solids at Room Temperature and Below", NBS Monograph 131 (1973).
10. "American Institute of Physics Handbook", McGraw-Hill, New York (1957).
11. L. Lockhart, NRL Private Communication (1978).
12. "Dielectric Materials and Applications", A. Von Hippel Ed., John Wiley & Sons, New York (1954).
13. M. A. Herlin and S. C. Brown, Phys. Rev. 74, 291, (1948).
14. S. C. Brown, in Encyclopedia of Physics, S. Flugge, Ed., Springer-Verlag, Berlin (1956), Vol. XXII.

15. A. D. MacDonald, D. V. Gaskell and H. N. Gitterman, Phys. Rev. 130, 1841 (1963).

16. C. DeMichelis, IEEE, J. Quantum Electron, QE-5, 188 (1969) and references therein.

17. N. Kroll and K. Watson, Phys. Rev. A 5, 1883 and references therein.

18. P. F. Browne, Proc. Phys. Soc. 86, 1323 (1965).

19. A. D. MacDonald, Proc. IRE, 47, 436 (1959).

20. R. W. Mink, J. Appl. Phys. 35, 252 (1964).

21. W. E. Scharfman, W. C. Taylor and T. Morita, IEEE, Tran., on Antenna and Propagation, 12, 1709 (1964) p. 709, Nov (1964). W. E. Scharfman and T. Morita, J. Appl. Phys. 33, 2016 (1964).

22. Y. A. Lupan, Sov. Phys. Tech. Phys. 21, 1367 (1976).

23. F. J. Mehr and M. A. Biondi, Phy. Rev. 181, 264 (1969).

24. M. Bortner and T. Baurer, Chapter 24, Defense Nuclear Agency Reaction Handbook, DNA 1948, Bortner and Baurer Eds. DASIAC DOD Nuclear Information and Analysis Center, GE-TEMPO, Santa Barbara (1972).

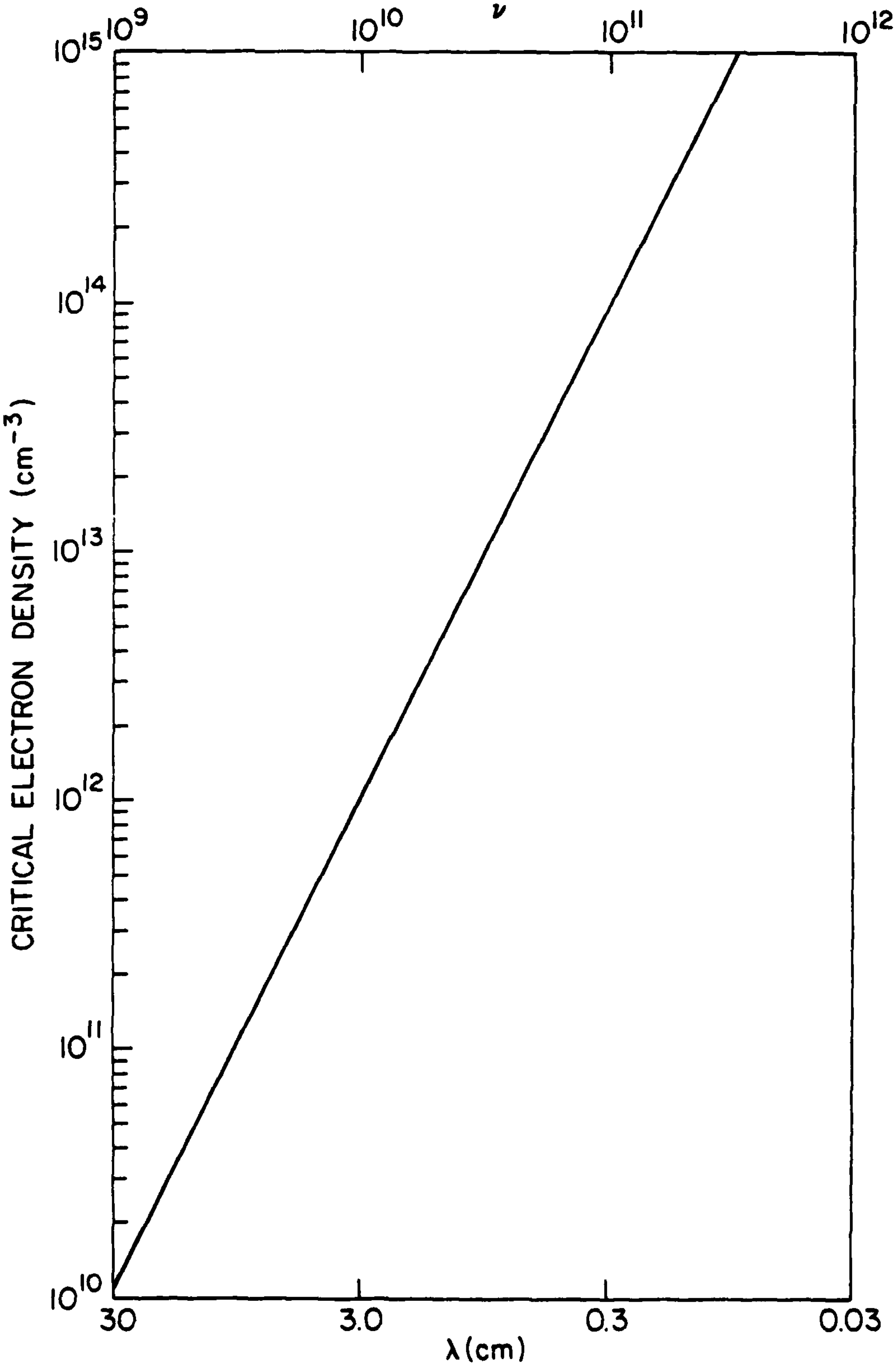

Fig. 3.1 — The critical plasma electron density as a function of the incident wavelength

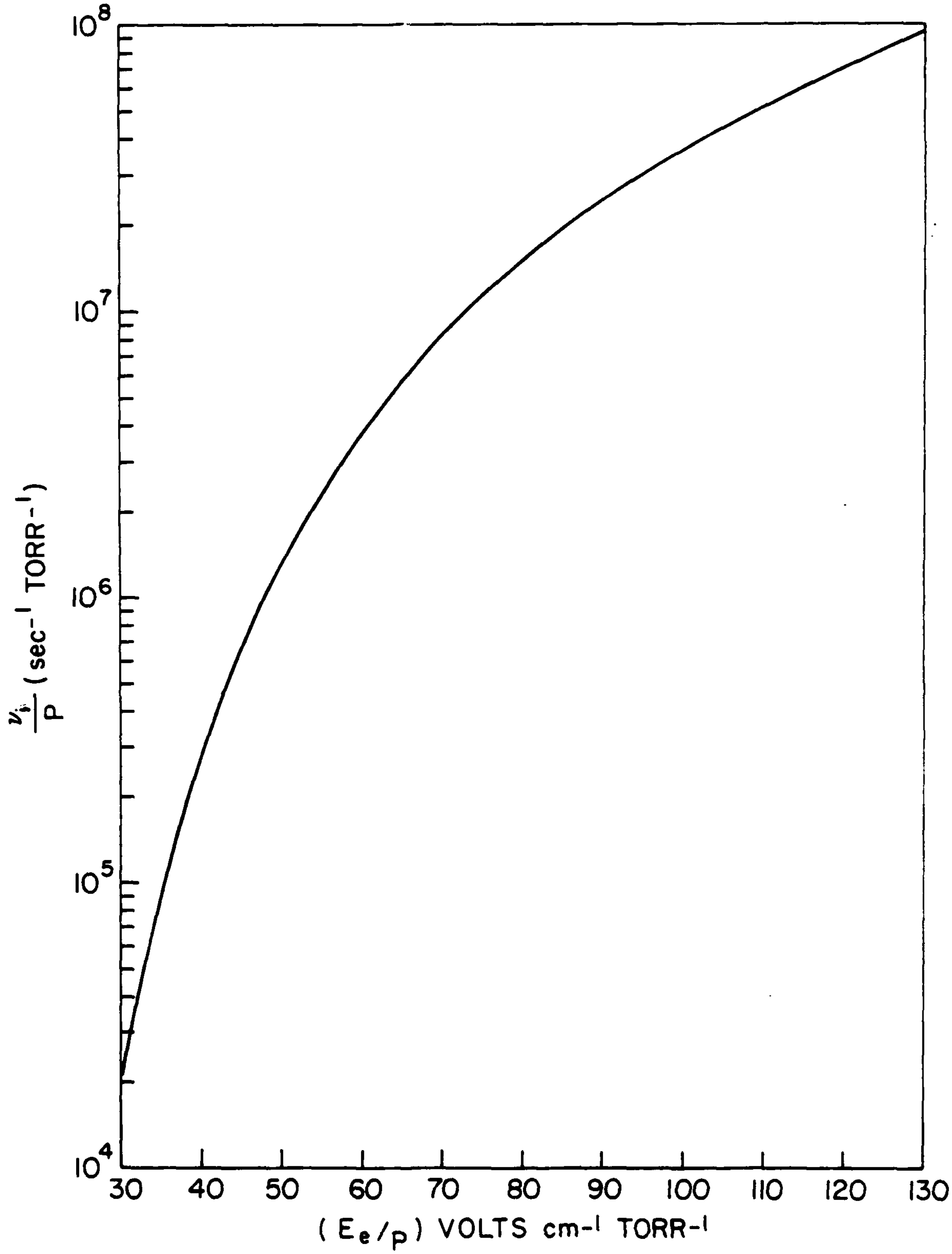

Fig. 3.2 — The ionization frequency of air per Torr as a function of the effective breakdown field per Torr

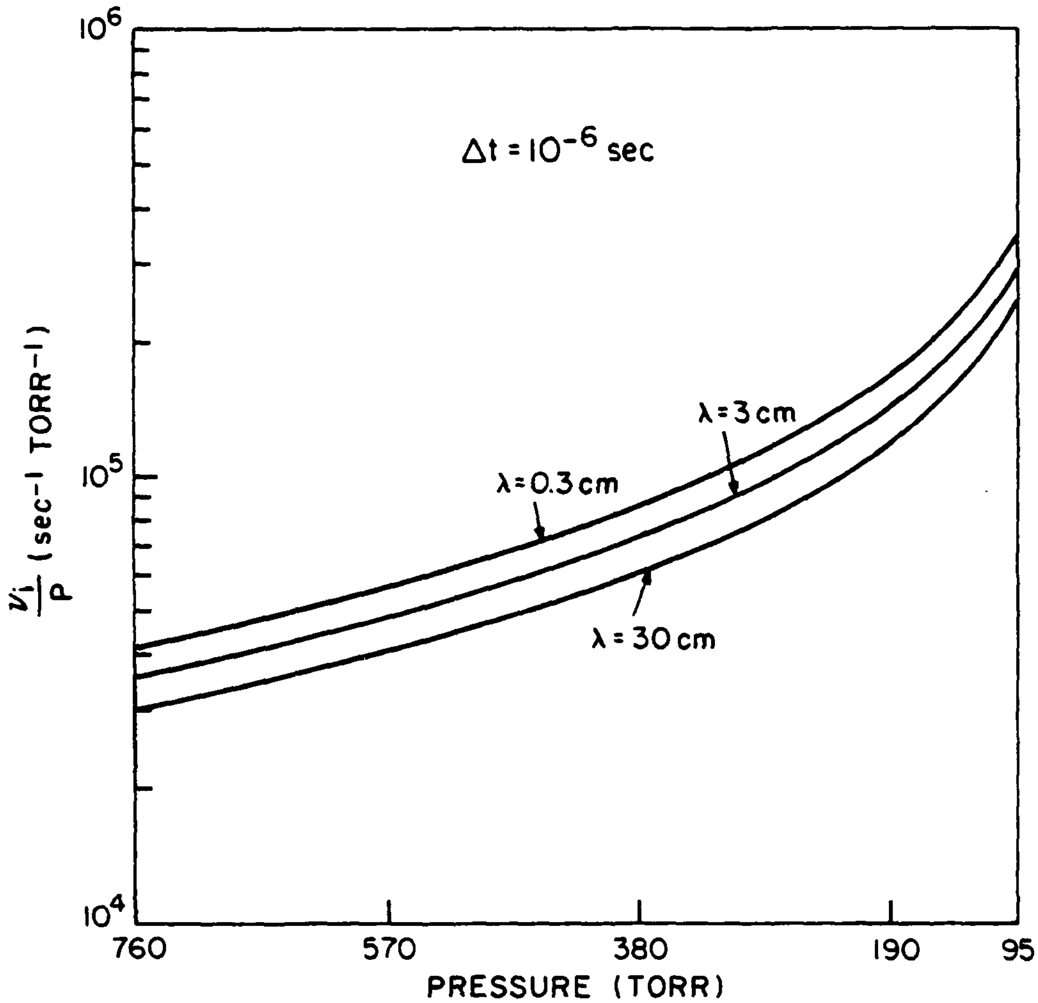

Fig. 3.3 — The ionization frequency per Torr as a function of pressure for several incident radiation wavelength and fixed pulse duration of 10^{-6} sec

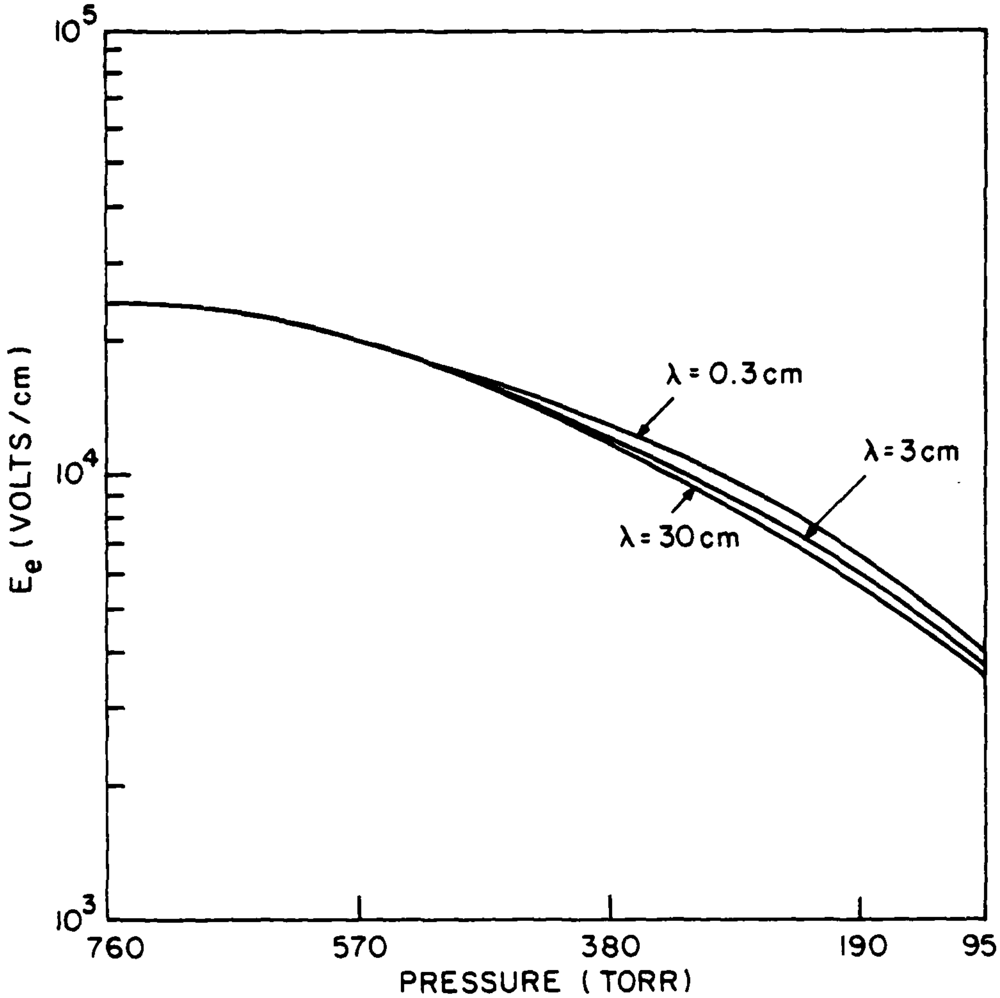

Fig. 3.4 — The corresponding effective breakdown field for the ionization frequencies of Fig. 3.3 as a function of pressure

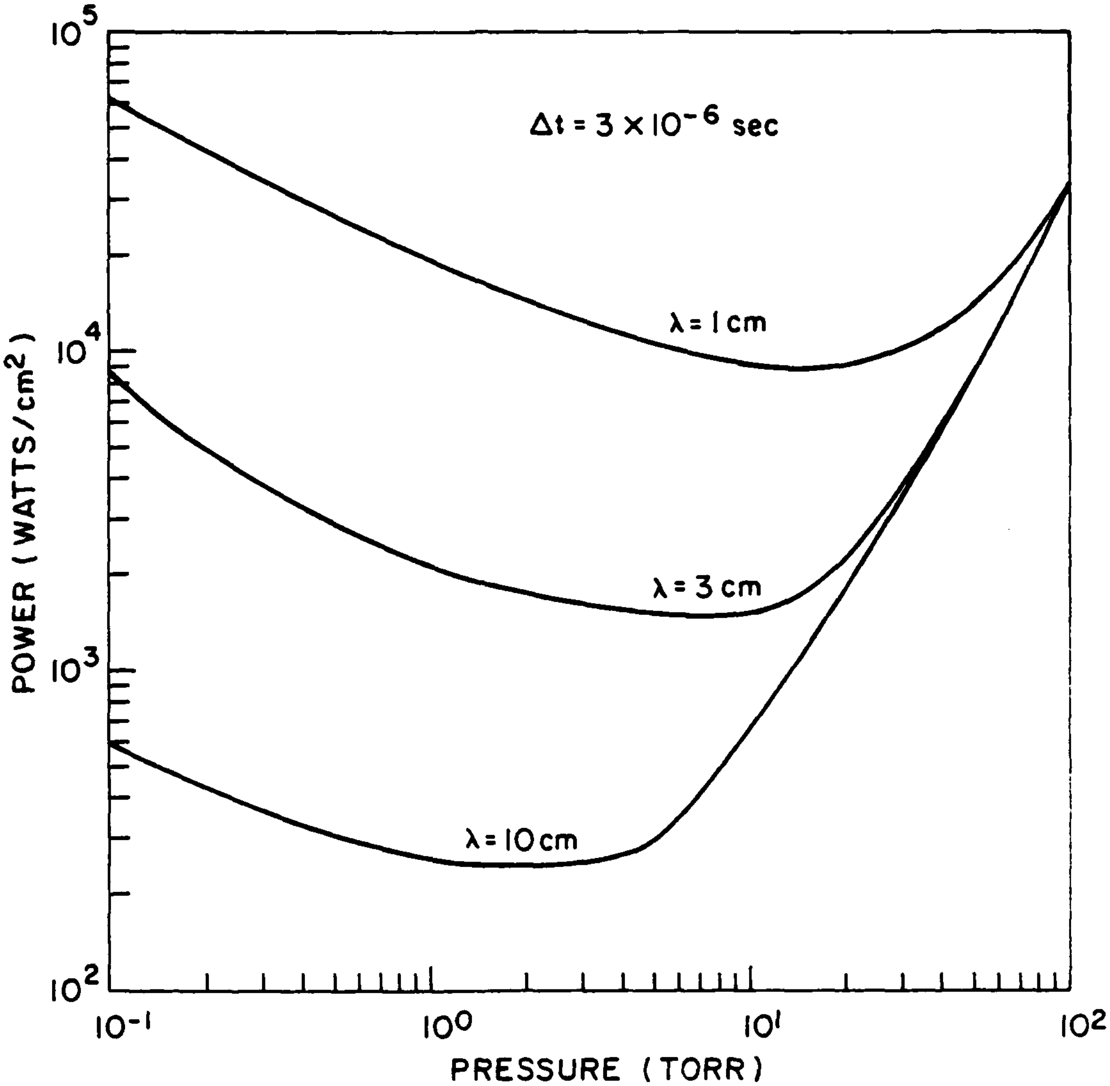

Fig. 3.5 — Threshold Breakdown Power as a function of pressure for several incident radiation wavelength and a fixed pulse duration of 3×10^{-6} sec

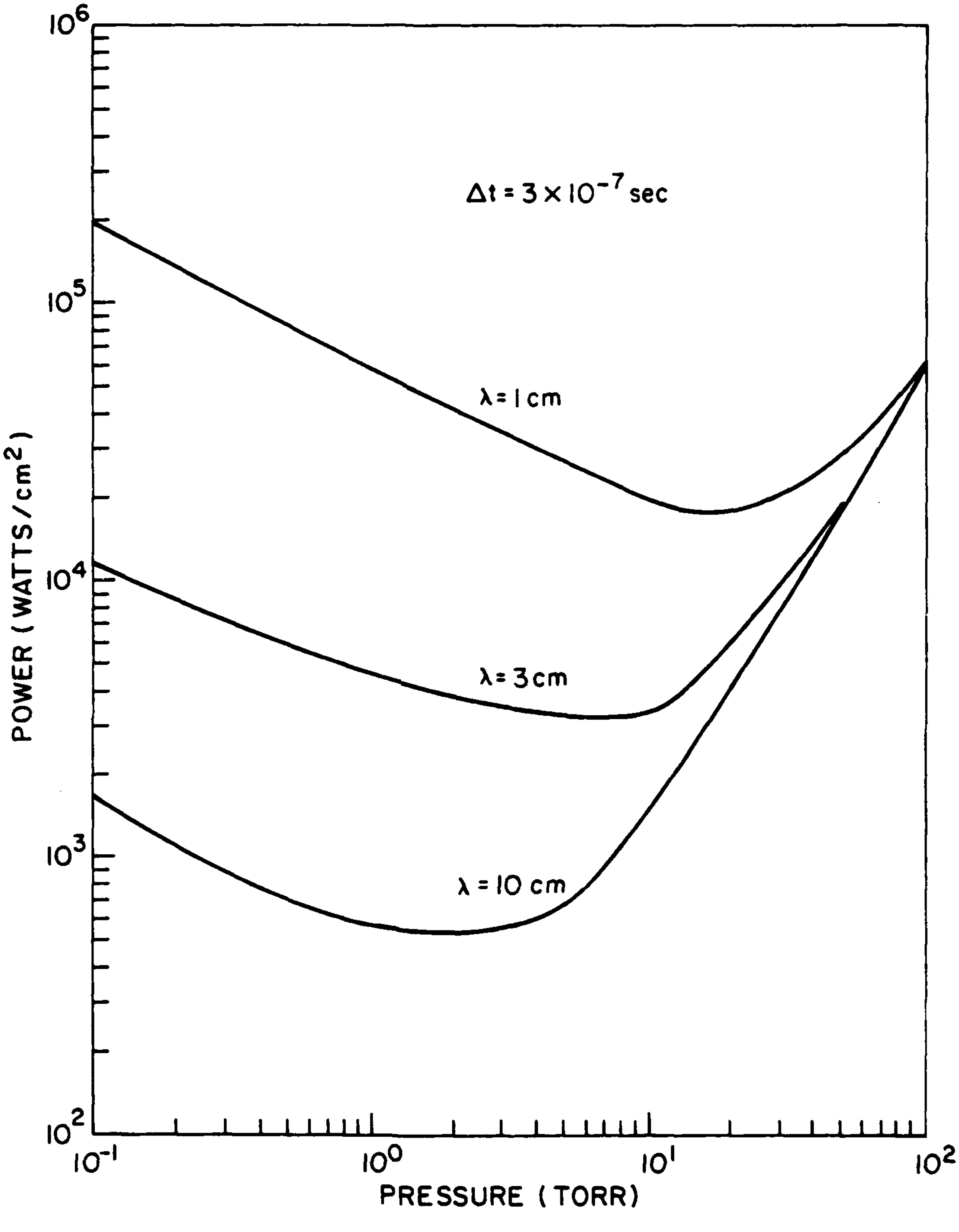

Fig. 3.6 — Threshold Breakdown Power as a function of pressure for several incident radiation wavelengths and a fixed pulse duration of 3×10^{-7} sec (compare with longer time of Fig. 3.5)

DISTRIBUTION LIST

DIRECTOR
Defense Advanced Research Project Agency
Architect Building
1400 Wilson Blvd.
Arlington, VA 22209
ATTN: Strategic Tech Office
Dr. J. Bayless
Dr. J. Mangano

Defense Technical Information Center
Cameron Station
Alexandria, VA 22314
ATTN: TC — 12 copies

DIRECTOR
Defense Intelligence Agency
Washington, DC 20301
ATTN: W. Wittig DC - 7D
DT-1B
P. Castleberry

B-K Dynamics, Inc.
15825 Shady Grove Rd.
Rockville, MD 20850
ATTN: Mr. I. Kuhn

CHIEF of Naval Research
Department of the Navy
Arlington, VA 22217
ATTN: Code 464, T. Berlincourt
Code 421, Dr. W. J. Condell

COMMANDING OFFICER
Naval Research Laboratory
Washington, DC 20375
ATTN: Code 4701, Jack D. Brown
Code 4700, Division Superintendent — 25 copies
Code 4700.1, Dr. A. W. Ali — 20 copies
Code 4777, Mr. I. M. Vitkovitsky
Code 4790, Dr. M. Lampe
Code 4740, Dr. V. Granatstein
Dr. R. Parker
Code 6330, Dr. T. J. Schriempf

COMMANDER
Naval Surface Weapons Center
White Oak, Silver Spring, MD 20910
ATTN: Code 1224, Navy Nuc Programs Office
Code 730, Tech. Lib.
Dr. C. M. Huddleston

AF Weapons Laboratory, AFSC
Kirtland AFB, NM 87117
ATTN: Maj. H. Dagliani
Dr. K. Dreyer
Lt. David L. Smith
Dr. D. Straw

AFTAC
Patrick AFB, FL 32925
ATTN: TF Maj. E. Hines
TF Capt. Wiley
TN

HQ USAF/RD
Washington, DC 20330
ATTN: RDQ

University of California
Lawrence Livermore National Laboratory
P. O. Box 808
Livermore, CA 94550
ATTN: Tech Info Dept L-3
R. Briggs

Naval Air Systems Command
Jefferson Plaza #1
Washington, DC 20361
ATTN: Dr. R. Wasneski

R & D Associates
P. O. Box 9695
Marina del Rey, CA 90291
ATTN: Robert E. Lelevier
Forest Gilmore

Sandia National Laboratory
P. O. Box 5800
Albuquerque, NM 87185
ATTN: R. B. Miller

Science Applications, Inc.
5 Palo Alto Square
Palo Alto, CA 94304
ATTN: Dr. R. Johnston

COMMANDER
U.S. Army Missile Command
Redstone Arsenal
Huntsville, AL 35809
ATTN: AMSMI-YTT W. G. Preussel, Jr.
P. Oliver